

Contamination in the Rare-Earth Element Orthophosphate Reference Samples

Volume 107

Number 6

November–December 2002

John J. Donovan

Department of Geological Sciences,
The University of Oregon,
Eugene, OR 97403-1272

John M. Hanchar

Department of Earth and Environmental
Sciences,
The George Washington University,
Washington, DC 20006

Phillip M. Picolli

Department of Geology,
The University of Maryland,
College Park, MD 20742

Marc D. Schrier

Department of Chemistry,
The University of California,
Berkeley, CA 94720

Lynn A. Boatner

Solid State Division, Oak Ridge
National Laboratory,
Oak Ridge, TN 37831

and

Eugene Jarosewich

Department of Mineral Sciences,
Smithsonian Institution,
Washington, DC 20560

donovan@oregon.uoregon.edu

Several of the fourteen rare-earth element (plus Sc and Y) orthophosphate standards grown at Oak Ridge National Laboratory in the 1980s and widely distributed by the Smithsonian Institution's Department of Mineral Sciences, are significantly contaminated by Pb. The origin of this impurity is the $\text{Pb}_2\text{P}_2\text{O}_7$ flux that is derived from the thermal decomposition of PbHPO_4 . The lead pyrophosphate flux is used to dissolve the oxide starting materials at elevated temperatures ($\approx 1360^\circ\text{C}$) prior to the crystal synthesis. Because these rare-earth element standards are extremely stable under the electron beam and considered homogenous, they have been of enormous value to electron probe micro-

analysis (EPMA). The monoclinic, monazite structure, orthophosphates show a higher degree of Pb incorporation than the tetragonal xenotime structure, orthophosphates. This paper will attempt to describe and rationalize the extent of the Pb contamination in these otherwise excellent materials.

Key words: EPMA; microanalysis; orthophosphates; quantitative analysis; rare earth elements; rare earth phosphates; REE; standards.

Accepted: August 22, 2002

Available online: <http://www.nist.gov/jres>

1. Introduction

Highly accurate analyses from the electron microprobe analyzer (EMPA) are only (but not solely) obtainable through the use of well-characterized and stable standards containing a major and/or known concentration of the element in question. For the rare earth elements (REE) this goal has, until recently, been elusive

due to the lack of specimens exhibiting these vital properties.

The lanthanide orthophosphates, consisting of compounds with the stoichiometry LnPO_4 where Ln represents any of the REE in the series extending from La to Lu (plus the related compounds YPO_4 and ScPO_4), are

chemically durable and radiation resistant refractory materials. During the early 1980s a variety of single crystal rare earth orthophosphate samples were synthesized at Oak Ridge National Laboratory and the structures determined from x-ray refinements [1, 2, 3, 4, 5, and 6]. The primary purposes of these studies were varied, but they included nuclear and actinide waste disposal and scintillator material research as well as fundamental materials characterization investigations. The crystals were synthesized using a high-temperature solvent (flux-growth) technique, the details of which are available from the original papers, and a good overview of the development of these orthophosphates is discussed in Boatner and Sales [7], and references therein.

One interesting fact is that although the starting materials were carefully selected to be free from REE impurities, they were grown in a lead pyrophosphate (PbHPO_4) flux. Pb contamination was not a concern for the original purposes of those experiments, however its presence was detected early on, and the solid state chemistry (but not the concentration) of Pb in the orthophosphate was characterized by means of electron paramagnetic resonance spectroscopy (EPR) [8]. Subsequently, these materials were investigated for possible use as standards for EPMA by the Smithsonian Institution [9], and put through a series of tests. These included homogeneity testing and a comparison to the commonly used REE doped aluminum silicate glass standards of Drake and Weill [10] using the EPMA, and a check of 10 selected REE contaminants on 7 of the compounds using instrumental neutron activation analysis. The materials appeared to be robust under electron bombardment, did not oxidize or seem hygroscopic, and no serious contamination or inhomogeneities were noted at the time and these efforts were followed by a general distribution of the material to interested parties.

In the late 1990s it was reported to one of us (JJD) that at least one investigator (E. J. Essene, University of Michigan, personal communication) had raised the issue of the role of the Pb impurity in some of the REE phosphate standards. The Pb impurity is especially significant in the CePO_4 crystals whose black coloration is consistent with possible mixed valence (Ce^{3+} – Ce^{4+}) effects—the presence of which could alter the high-temperature solid-state chemical properties and lead to an enhanced incorporation of Pb during the crystal-growth process. Subsequent investigations of the materials revealed Pb ranging in concentration from less than 0.01 mass fraction to more than 0.04 mass fraction in the CePO_4 , depending on the specific grains analyzed. It is the intent of this paper to characterize the extent of the Pb contamination in these otherwise extremely useful standards for EPMA.

2. Experimental Methods

Quantitative wavelength dispersive spectrometry (WDS) analyses for the REEs Sc, Y, and Pb in each of the 16 orthophosphate samples were done using a Cameca SX-51¹ electron microprobe at 20 keV, 20 nA (2.0×10^{-8} A), using a 10 μm beam diameter at UC Berkeley. In addition, one of the Drake and Weill REE glasses [10], and two other REE doped calcium aluminum silicate discussed in Roeder [11] and Roeder et al. [12] were analyzed. For quantitative analyses, the K_α x-ray line was used for Sc, L_α lines for Y and the other REE elements, and the M_α line was used for Pb. Count times were 20 s on peak and 10 s on each off-peak position except for Pb where the count times were doubled, respectively.

A complete description of the analytical setup and secondary standard accuracy for the analyzed elements (the composition of the REE phosphate primary standards in these cases had been previously adjusted for average Pb concentrations) is presented in Table 1. Secondary standards included synthetic yttrium-aluminum garnet (YAG) and alamosite (PbSiO_3) from Tsumeb, Namibia and were assumed to be stoichiometric for Y and Pb, respectively. The Roeder REE glass S-254 [12] was assumed to have a nominal concentration (1.04×10^{-2} mass fraction) for La, Ce, Pr, Nd, Sm, Dy, Ho, Er, Yb, and Lu, and the Drake and Weill REE-1 glass was used based on published concentrations for Eu, Gd, Tb, and Tm [10]. For all rare-earth elements, the relative differences obtained when comparing the secondary standards to the primary standard is better than 10 % at the 0.01 mass fraction to 0.04 mass fraction concentration levels and better than 6 % in all but three cases (Pr, Sm and Lu).

The difficulty of dealing with interfering elements for REE analyses using the L_α x-ray lines is painfully evident in even cursory WDS spectral scans on these samples and can only be overcome by careful and consistent application of an automatic correction scheme. Table 2 shows the REEs that interfere with the analyzed elements. These were interferences quantitatively corrected for using the iteration method of Donovan et al. [13], that is especially well suited for using large magnitude interferences for trace element determinations. For the Pb analyses, the M_α line was used with a quantitative interference correction for Y (possible high order interferences from La and Tb were not observed). Standard

¹ NIST disclaimer: Certain commercial equipment, instruments, or materials are identified in this paper to foster understanding. Such identification does not imply recommendation or endorsement by the National Institute of Standards and Technology, nor does it imply that the materials or equipment identified are necessarily the best available for the purpose.

Table 1. Analytical setup and measured differences between the secondary standards and the primary standard for REE quantitative analysis^a

Element Sc K _α	Spect. setup LiF (FPC-2)	Primary standard ScPO ₄ (syn.)	Secondary standard Conc in mass fraction × 10 ²	Relative diff.
YL _α	PET (FPC-1)	YPO ₄ (syn.)	YAG (stoic.)	+0.368, +0.82 %
LaL _α	LiF (FPC-2)	LaPO ₄ (syn.)	S-254 (1.04 nom.)	−0.020, −1.92 %
CeL _α	LiF (FPC-2)	CePO ₄ (syn.)	S-254 (1.04 nom.)	−0.010, −0.95 %
PrL _α	LiF (FPC-2)	PrPO ₄ (syn.)	S-254 (1.04 nom.)	−0.103, −9.95 %
NdL _α	LiF (FPC-2)	NdPO ₄ (syn.)	S-254 (1.04 nom.)	−0.007, −0.70 %
SmL _α	LiF (FPC-2)	SmPO ₄ (syn.)	S-254 (1.04 nom.)	−0.055, −5.27 %
EuL _α	LiF (FPC-2)	EuPO ₄ (syn.)	REE-1 (3.63 pub.)	+0.069, +1.90 %
GdL _α	LiF (FPC-2)	GdPO ₄ (syn.)	REE-1 (3.87 pub.)	−0.012, −0.31 %
TbL _α	LiF (FPC-2)	TbPO ₄ (syn.)	REE-1 (3.78 pub.)	−0.116, −3.08 %
DyL _α	LiF (FPC-2)	DyPO ₄ (syn.)	S-254 (1.04 nom.)	−0.035, −3.35 %
HoL _α	LiF (FPC-2)	HoPO ₄ (syn.)	S-254 (1.04 nom.)	−0.041, −3.92 %
ErL _α	LiF (FPC-2)	ErPO ₄ (syn.)	S-254 (1.04 nom.)	−0.047, −4.51 %
TmL _α	LiF (FPC-2)	TmPO ₄ (syn.)	REE-1 (3.81 pub.)	−0.127, −3.33 %
YbL _α	LiF (FPC-2)	YbPO ₄ (syn.)	S-254 (1.04 nom.)	−0.047, −4.53 %
LuL _α	LiF (FPC-2)	LuPO ₄ (syn.)	S-254 (1.04 nom.)	−0.103, −9.94 %
PbM _α	PET (FPC-1)	PbCO ₃ (Tsumeb)	PbSiO ₃ (stoic.)	+0.550, +0.75 %

^a Analytical spectrometer setup (flow proportional detectors: FPC-1 indicates 1 atm P-10 and FPC-2 indicates 2 atm P-10) for REE elements (plus Sc, Y, and Pb) and results of secondary standard measurements (algebraic difference and relative difference) performed at UC Berkeley. All elements were measured at 20 keV, 20 nA (150 nA for the four grain map), 10 μm beam diameter, 20 s on-peak integration time and 10 s on each off-peak except for Pb which was counted for 40 s on-peak and 20 s on each off-peak position (240 s on-peak and 120 s on each off-peak position for the four grain map in Fig. 5). Each result shown is the average of 10 measurements.

and background intensities along with the calculated P/B (peak to background) for each line in its associated primary standard are shown in Table 3.

Under the analytical conditions which were utilized at Berkeley, the minimum detection limits for both single analyses calculated from Love and Scott [14], and for the average of 10 replicate analyses based on Goldstein et al. [15], are shown in Table 4. Minimum detection limits for 10 replicate analyses based on the actual measured standard deviation are about 3.0×10^{-4} mass fraction to 6.0×10^{-4} mass fraction for all elements in all matrices although only values for CePO₄ or GdPO₄ are shown in Table 4. A measured detection limit of 3×10^{-4} mass fraction to 6×10^{-4} mass fraction for the average of 10 replicates at 99 % a confidence level was typical for the REE analyses under these conditions. The Pb detection limit at a 99 % confidence level was about 4.5×10^{-4} mass fraction.

Another set of measurements, for the analysis of Pb homogeneity only, were also done on the same grains, but in a different area from the REE and Pb measurements done at UC Berkeley. These measurements were made for each REE orthophosphate using a JEOL 8900 Superprobe at the University of Maryland-College Park. X-ray intensities of Pb were obtained using an accelerating voltage of 20 keV, and a beam current of 150 nA. Count times were 60 s on peak, and 30 s for backgrounds on each side of the peak. Pb was analyzed using a PETH (which utilizes a smaller diameter Rowland Circle allowing for higher count rates, but has poorer

wavelength resolution) crystal, and background positions of +4 mm ($L = 173.307$ mm or 5.4013 Å) and −3 mm ($L = 166.307$ mm or 5.1828 Å). Natural cerussite (PbCO₃) from Tsumeb, Namibia, was used as a standard for Pb (0.8393 mass fraction PbO). It should be noted that although cerussite is a carbonate mineral it did not appear to degrade under the electron beam during the analyses. The Pb M_α x-ray line was used for all analyses, with the exception of YPO₄, where M_β was used due to an interference from Y₁₇₃ on Pb M_α. For these Pb homogeneity measurements, the REE and phosphate concentrations were not measured but were incorporated as stoichiometric proportions into the ZAF algorithm in order to approximately account for matrix effects. The single analysis detection limit at a 99 % confidence level for Pb under these analytical conditions was about 1.4×10^{-4} mass fraction Pb based on a standard count rate of 263.9 cps/nA and a background of 0.8 cps/nA measured on CePO₄.

Measurements were done on two different sets of REE orthophosphate samples. The first set consists of material for 16 orthophosphates, including Sc and Y obtained from one of us (JMH) and mounted along with primary and secondary standards for analysis and interference corrections. These materials were mounted in a 25 mm diameter acrylic mount approximately 1.5 cm deep using a cold set epoxy and circulated to both laboratories. This sample will be referred to as the “Round Robin” mount in the discussion that follows.

Table 2. Quantitative interferences.^a Also listed are the wavelengths (in Å) of the x-ray lines

Element Å	On peak interferences Å
ScK _α at 3.0320	ErL _{β2} (II) at 3.0284
YL _α at 2.6657	LaL _{γ1} (III) at 6.4260 (not observed)
LaL _α at 2.6657	NdL _I (I) at 2.6766
CeL _α at 2.5615	
PrL _α at 2.4630	LaL _{β1,4} (I) at 2.4595, 2.4595 SmL _I (I) at 2.4826
NdL _α at 2.3704	CeL _{β1,4} (I) at 2.3566, 2.3499 PbL _{α1,2} (II) at 2.3504, 2.3732
SmL _α at 2.1998	CeL _{β2} (I) at 2.2092 PrL _{β3} (I) at 2.2175 (not observed)
EuL _α at 2.1209	NdL _{β3} (I) at 2.1273 PrL _{β2} (I) at 2.1197
GdL _α at 2.0468	CeL _{γ1} (I) at 2.0489 LaL _{γ2,3} (I) at 2.0462, 2.0415 NdL _{β2} (I) at 2.0365
TbL _α at 1.9765	LaL _{γ4} (I) at 1.9834 PrL _{γ1} (I) at 1.9614 (not observed) SmL _{β3} (I) at 1.9627 (not observed)
DyL _α at 1.9088	PbL _{β1,2} (II) at 1.9660, 1.9650 (not observed) EuL _{β1,4} (I) at 1.9207, 1.9258 YbL _I (I) at 1.8946 (possibly observed)
HoL _α at 1.8450	GdL _{β1,4} (I) at 1.8472, 1.8543 LuL _I (I) at 1.8362 (not observed)
ErL _α at 1.7842	TbL _{β1,4} (I) at 1.7770, 1.7867 NdL _{γ2,3} (I) at 1.8015, 1.7968
TmL _α at 1.7268	DyL _{β1,4} (I) at 1.7110, 1.7212 GdL _{β2} (I) at 1.7457 SmL _{γ1} (I) at 1.7275
YbL _α at 1.6718	EuL _{γ1} (I) at 1.6577 SmL _{γ2} (I) at 1.6608 TbL _{β2} (I) at 1.6834 YK _{α1} (II) at 1.6580 (possibly observed)
LuL _α at 1.6195	HoL _{β4} (I) at 1.6597 (not observed) HoL _{β3} (I) at 1.6207 DyL _{β2} (I) at 1.6241
PbM _α at 5.2860	GdL _{γ1} (I) at 1.5928 (possibly observed) YL _{γ3} (I) at 5.2848 LaL _{α1} (II) at 5.3326 (not observed) TbL _{β1} (III) at 5.3310 (not observed)

^a Analyzed elements and interfering elements were quantitatively corrected by using the iteration method of Donovan et al. [12]. Many of these interferences are 1st order interferences and therefore are the same energy as the interfering line, and hence, cannot be reduced by the use of pulse height analysis (PHA). Selection of alternative (beta) lines is sometimes possible, but the resulting reduction in intensity will also reduce sensitivity.

The “Round Robin” mount was carefully analyzed for Pb at both Berkeley and College Park to check for inter-laboratory differences since the analytical results of trace element measurements are extremely sensitive to differences in spectrometer resolution and placement of off-peak intensity measurement positions. Homogeneity measurements were also done on this mount at College Park to check for possible Pb variations within this material itself.

Additional Pb measurements were performed at UC Berkeley on other material that was originally resident in the laboratory standard collection to check for possible inter-batch differences in Pb contamination some of the material had been produced in several runs at Oak Ridge under possibly different growth conditions. Analyses on this material will be referred to as the “Berkeley” REE mount.

Table 3. Standard peak and background intensities (linear interpolation method)^a

Element	Peak intensity (cps/nA)	Background intensity (cps/nA)	Peak/Background
ScK _α	49.3 (ScPO ₄)	0.2	246.5
YL _α	68.3 (YPO ₄)	0.5	136.6
LaL _α	38.5 (LaPO ₄)	0.3	128.3
CeL _α	45.4 (CePO ₄)	0.5	90.8
PrL _α	55.1 (PrPO ₄)	0.6	91.8
NdL _α	64.9 (NdPO ₄)	0.6	108.1
SmL _α	80.8 (SmPO ₄)	1.3	62.2
EuL _α	89.6 (EuPO ₄)	1.1	81.5
GdL _α	95.2 (GdPO ₄)	1.2	79.3
TbL _α	101.9 (TbPO ₄)	1.3	78.4
DyL _α	107.8 (DyPO ₄)	1.5	71.9
HoL _α	113.6 (HoPO ₄)	2.2	51.6
ErL _α	119.5 (ErPO ₄)	2.1	56.9
TmL _α	122.9 (TmPO ₄)	2.5	49.2
YbL _α	128.0 (YbPO ₄)	2.6	49.2
LuL _α	131.3 (LuPO ₄)	3.4	38.6
PbM _α	72.0 (PbCO ₃)	0.6	120.0

^a Average peak and background intensities measured on the primary standards for the analyzed elements along with calculated peak to background ratios. Off-peak positions were based on high-resolution spectral scans of the low to high off-peak regions of each REE element and Pb in each of the REE phosphates. The purpose was to avoid off-peak interferences as much as possible.

Table 4. Typical single analysis and average (replicate) detection limits^a

Element	Detection limit (single point) (.99 CL) (mass fraction × 10 ² in CePO ₄)	Detection limit (avg. of 10) (.99 CL) (mass fraction × 10 ² in CePO ₄)
ScK _α	0.058	0.018
YL _α	0.103	0.024
LaL _α	0.187	0.045
CeL _α	0.147 (in GdPO ₄)	0.050 (in GdPO ₄)
PrL _α	0.104	0.058
NdL _α	0.111	0.068
SmL _α	0.103	0.042
EuL _α	0.137	0.052
GdL _α	0.097	0.125 ^b
TbL _α	0.139	0.046
DyL _α	0.100	0.033
HoL _α	0.140	0.042
ErL _α	0.097	0.042
TmL _α	0.139	0.033
YbL _α	0.139	0.038
LuL _α	0.142	0.043
PbM _α	0.077 (in GdPO ₄)	0.045 (in GdPO ₄)

^a Single point analysis detection limits in a matrix of CePO₄ at a 99 % confidence level (CL). A GdPO₄ matrix for Ce and Pb was used since Ce is a major element in CePO₄ and Pb was determined to be inhomogeneous in the CePO₄. CL and averaged detection limits for the same matrices at 99 % confidence interval based on the actual measured standard deviation of 10 measurements on each standard are reported.

^b Gd is possibly present as very small, widely dispersed concentrations in the CePO₄ which could explain this unusually high calculated detection limit (for example the calculated average detection limit for GdL_α in DyPO₄ is 0.07 mass fraction × 10²).

3. Results and Discussion

3.1 REE Impurities in the Orthophosphate Standards

Table 5 shows the trace REE elements measured in each of the orthophosphates at UC Berkeley on the

“Round Robin” mount. One can see that as stated in the original paper by Jarosewich and Boatner [9], the material is generally very pure based on quantitative results from instrumental neutron activation analysis (INAA). The only statistically significant REE contamination anomalies we observed were the presence of approximately 9×10^{-4} mass fraction Eu in GdPO₄ (Jarosewich

Table 5. Trace Pb and REE concentrations in the REEPO₄ standards^a (concentrations and uncertainties in mass fraction × 10²)

USNM #	ScPO ₄ 168495	YPO ₄ 168499	LaPO ₄ 168490	CePO ₄ 168484	PrPO ₄ 168493	NdPO ₄ 168492	SmPO ₄ 168494	EuPO ₄ 168487
ScK _α		.01 ± .01	.01 ± .02	.01 ± .01	.01 ± .01	.01 ± .01	.01 ± .01	.00 ± .00
YL _α	.01 ± .02		.01 ± .01	.01 ± .01	.00 ± .01	.02 ± .03	.01 ± .02	.00 ± .00
LaL _α	.01 ± .01	.02 ± .03		.00 ± .00	.03 ± .05	.02 ± .04	.03 ± .03	.01 ± .01
CeL _α	.00 ± .01	.05 ± .06	.01 ± .01		.03 ± .04	.03 ± .04	.03 ± .04	.02 ± .02
PrL _α	.03 ± .03	.01 ± .02	.07 ± .13 ^b	.02 ± .03		.00 ± .01	.01 ± .01	.02 ± .03
NdL _α	.00 ± .00	.01 ± .02	.00 ± .01	.01 ± .02	.01 ± .03		.00 ± .01	.04 ± .04
SmL _α	.02 ± .03	.01 ± .02	.01 ± .02	.02 ± .04	.01 ± .02	.00 ± .00		.01 ± .02
EuL _α	.02 ± .03	.01 ± .02	.03 ± .03	.00 ± .01	.08 ± .11 ^b	.03 ± .05	.03 ± .02	
GdL _α	.02 ± .03	.02 ± .03	.03 ± .06	.04 ± .05	.01 ± .03	.02 ± .03	.00 ± .00	.02 ± .05
TbL _α	.01 ± .01	.02 ± .03	.02 ± .03	.00 ± .01	.03 ± .04	.00 ± .00	.03 ± .05	.00 ± .01
DyL _α	.03 ± .02	.02 ± .02	.03 ± .04	.02 ± .03	.00 ± .00	.00 ± .00	.00 ± .00	.02 ± .03
HoL _α	.01 ± .02	.01 ± .02	.02 ± .03	.02 ± .03	.00 ± .00	.00 ± .01	.00 ± .00	.00 ± .00
ErL _α	.03 ± .03	.02 ± .02	.02 ± .03	.03 ± .04	.00 ± .00	.02 ± .03	.07 ± .04	.00 ± .00
TmL _α	.02 ± .02	.01 ± .02	.02 ± .02	.01 ± .02	.02 ± .03	.02 ± .02	.06 ± .07	.06 ± .06
YbL _α	.00 ± .00	.03 ± .04	.02 ± .03	.04 ± .05	.04 ± .04	.03 ± .03	.02 ± .03	.02 ± .03
LuL _α	.02 ± .03	.01 ± .03	.01 ± .02	.03 ± .04	.02 ± .03	.04 ± .03	.00 ± .00	.00 ± .01
PbM _α	.00 ± .00	.01 ± .01	1.05 ± .17	1.68 ± .07	.77 ± .04	.60 ± .03	.99 ± .07	.52 ± .06

	GdPO ₄ 168488	TbPO ₄ 168496	DyPO ₄ 168485	HoPO ₄ 168489	ErPO ₄ 168486	TmPO ₄ 168497	YbPO ₄ 168498	LuPO ₄ 168491
ScK _α	.01 ± .01	.00 ± .00	.01 ± .01	.01 ± .02	.01 ± .02	.00 ± .00	.00 ± .01	.01 ± .02
YL _α	.01 ± .02	.01 ± .02	.07 ± .05	.02 ± .03	.02 ± .03	.01 ± .01	.04 ± .03	.03 ± .03
LaL _α	.02 ± .04	.01 ± .02	.02 ± .04	.03 ± .04	.01 ± .02	.01 ± .01	.03 ± .05	.02 ± .03
CeL _α	.03 ± .04	.01 ± .02	.02 ± .02	.01 ± .03	.03 ± .04	.01 ± .01	.01 ± .02	.01 ± .02
PrL _α	.01 ± .02	.01 ± .03	.01 ± .02	.02 ± .03	.02 ± .04	.01 ± .03	.02 ± .05	.01 ± .02
NdL _α	.01 ± .02	.02 ± .03	.01 ± .02	.01 ± .03	.02 ± .04	.03 ± .04	.00 ± .00	.03 ± .04
SmL _α	.02 ± .03	.00 ± .01	.03 ± .04	.00 ± .01	.02 ± .02	.03 ± .03	.03 ± .03	.02 ± .03
EuL _α	.09 ± .06	.03 ± .03	.00 ± .01	.00 ± .01	.01 ± .03	.01 ± .01	.01 ± .02	.01 ± .01
GdL _α		.01 ± .02	.01 ± .02	.00 ± .01	.00 ± .00	.02 ± .02	.02 ± .03	.01 ± .01
TbL _α	.01 ± .02		.02 ± .03	.01 ± .01	.00 ± .00	.02 ± .03	.02 ± .03	.01 ± .03
DyL _α	.00 ± .00	.00 ± .00		.00 ± .00	.02 ± .04	.00 ± .00	.06 ± .05	.01 ± .03
HoL _α	.14 ± .21 ^b	.01 ± .02	.11 ± .06		.01 ± .01	.01 ± .03	.02 ± .04	.03 ± .03
ErL _α	.00 ± .00	.05 ± .09	.01 ± .02	.00 ± .00		.11 ± .07	.02 ± .02	.00 ± .01
TmL _α	.01 ± .02	.00 ± .00	.03 ± .05	.03 ± .03	.00 ± .00		.00 ± .01	.04 ± .04
YbL _α	.01 ± .01	.02 ± .03	.00 ± .01	.00 ± .00	.03 ± .04	.00 ± .00		.00 ± .00
LuL _α	.09 ± .07	.02 ± .03	.02 ± .05	.05 ± .07	.00 ± .00	.01 ± .04	.00 ± .00	
PbM _α	.49 ± .07	.02 ± .02	.02 ± .03	.02 ± .03	.02 ± .02	.01 ± .02	.02 ± .03	.04 ± .04

^a Average trace analyses of REE elements plus Sc, Y, and Pb for the USNM REE phosphates in the “Round Robin” mount measured at Berkeley. The quoted uncertainty is the measured one standard deviation value for 10 measurements.

^b Large magnitude interference corrections resulting in increasing uncertainty at trace levels. The apparent concentrations and large standard deviations for these three cases could be greatly reduced by using longer acquisition times on the unknown and the standard used for the interference correction.

and Boatner reported 1.9×10^{-5} mass fraction Eu in GdPO₄ using INAA), 1.1×10^{-3} mass fraction Ho and 7×10^{-4} mass fraction Y in the DyPO₄ (Jarosewich and Boatner reported 2.47×10^{-3} Ho in DyPO₄ using INAA, Y was not analyzed by INAA), and approximately 1.1×10^{-3} mass fraction Er in the TmPO₄ (Er was not analyzed by Jarosewich and Boatner with INAA). It is difficult to obtain commercially available REE oxide materials that are completely free of other REE impurities due to the nature of the starting materials (REE-rich phosphate and carbonate minerals) that

must be processed to extract individual REEs. The apparent concentration of 0.0009 ± 0.0007 mass fraction Lu in GdPO₄ is possibly due to an interference of Gd L_{γ1} at 1.5928 Å and the 0.0006 ± 0.0005 mass fraction Dy in YbPO₄ is possibly due to an interference of Yb L_I at 1.8946 Å and finally the 0.0004 ± 0.0003 mass fraction Yb in YPO₄ is possibly due to an interference of Y K_{α1} (II) at 1.658 Å. No other interferences could be invoked to explain the other apparent REE concentrations shown in bold in the table.

3.2 Pb Impurities in the Orthophosphate Standards

The results for Pb in the last row of Table 5 reveal that Pb is present from almost 0.02 mass fraction down to about 0.005 mass fraction element in seven of the REE orthophosphates in the “Round Robin” mount (in order of decreasing concentration: CePO₄, LaPO₄, SmPO₄, PrPO₄, NdPO₄, EuPO₄, and GdPO₄). The remaining REE orthophosphates did not contain Pb concentrations above the UC Berkeley detection limit of 4.5×10^{-4} mass fraction. These measurements consisted of a 10-point traverse on a single grain of each REE orthophosphate. Table 6 shows the Pb homogeneity measurements on the same “Round Robin” mount but performed in College Park with increased sensitivity (longer count times and higher beam currents). The two data sets agree well considering the apparent inhomogeneity of the Pb contaminated materials.

What is striking is that the Pb content varies considerably not only within each grain, but even more so from grain to grain, as seen in Table 7 where a number of Pb measurements (13-16) over the face of the four CePO₄ grains in the “Berkeley” mount show tremendous variation between grains from about 0.015 mass fraction to 0.045 mass fraction element.

3.3 Crystal Structure and Pb Contamination

Lead is present in significant amounts only in the monoclinic, high-temperature, monazite-structure orthophosphates (LaPO₄ through GdPO₄), and is absent, or nearly so, in the tetragonal, xenotime-structure, compounds (TbPO₄ through LuPO₄ and ScPO₄ and YPO₄) as can be seen in Fig. 1, where Pb concentration is plotted as a function of REE atomic number. Boatner and Sales [7] showed that there is a distinct structural change (monoclinic to tetragonal) between GdPO₄ and TbPO₄ which suggests that the incorporation of Pb in the monazite structure, and the lack of Pb incorporation in the xenotime structure orthophosphates, is related to this change in structure. The so-called lanthanide contraction is a continuous decrease in size across the REEs, and may also play a role in this, however, there are no abrupt decreases in the trivalent ionic radii across the REE series (including from Gd to Tb). Our data suggest that the exclusion of the large (e.g., 1.29 Å in eight coordination, [16] divalent lead cation is limited by the space available in the heavy REEO₈ (HREEO₈) polyhedra and that the divalent Pb ion, or the trivalent HREEs, will not fit easily into the xenotime structure. For the monoclinic orthophosphates, the light REEO₉ (LREEO₉) polyhedra is much larger and can accommodate the divalent Pb²⁺ ion into the xenotime structure [16].

Table 6. Pb (mass fraction $\times 10^2$) in the “round robin” mount measured in College Park^a

	ScPO ₄	YPO ₄ ^b	LaPO ₄	CePO ₄	PrPO ₄	NdPO ₄	SmPO ₄	EuPO ₄
PbM _α	.00 ± .00	.00 ± .00	.90 ± .32	1.90 ± .07	.92 ± .04	.86 ± .17	.86 ± .13	.64 ± .16
	GdPO ₄	TbPO ₄	DyPO ₄	HoPO ₄	ErPO ₄	TmPO ₄	YbPO ₄	LuPO ₄
PbM _α	.39 ± .16	.00 ± .00	.00 ± .00	.00 ± .00	.00 ± .00	.00 ± .00	.00 ± .00	.00 ± .00

^a Averaged mass fraction $\times 10^2$ results of Pb contamination measurements performed in College Park on the “round robin” mount. The mass fraction detection limit (99 % confidence level) was approximately 140×10^{-6} . Note that the measured Pb standard deviations for the uncontaminated materials are significantly smaller than the measurements performed at Berkeley. These results are due to the increased beam current and counting time used at College Park.

^b PbM_β was used to avoid the Y₁₇₃ line.

Table 7. Pb grain to grain variation within the CePO₄ material in the “Berkeley” mount^a

	Average (concentrations in mass fraction $\times 10^2$)	Standard deviation	Minimum	Maximum
Grain #1	2.68	0.45	2.04	3.47
Grain #2	2.55	0.16	2.33	2.83
Grain #3	1.54	0.04	1.48	1.59
Grain #4	3.64	0.46	3.08	4.50

^a Average and standard deviations (13-16 points over the face of each grain) of four grains from the “Berkeley” mount mapped in Fig. 1 in elemental mass fraction $\times 10^2$. Analytical conditions were 20 keV, 150 nA, and a 10 μm diameter beam. Each analysis is the average of 13 to 16 measurements distributed over the face of each grain. Only grain #3 was relatively homogeneous in Pb.

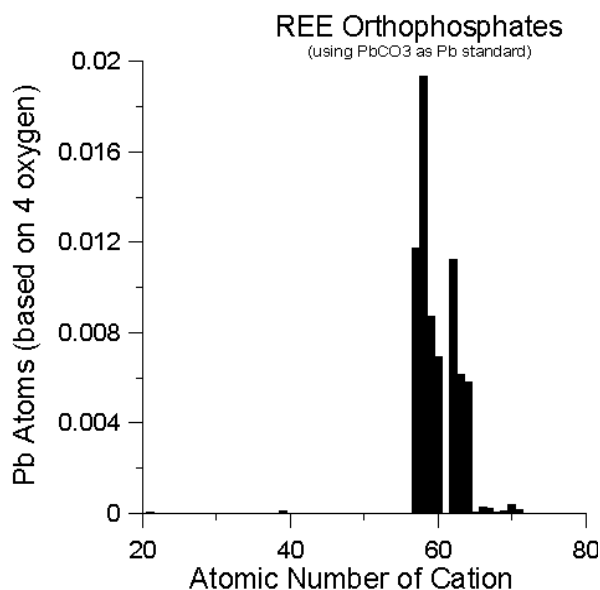


Fig. 1. Plot of Pb atoms (based on four oxygens) versus atomic number of the REE cation. Element 61 (Pm) is unstable and the orthophosphate is not available, therefore no measurement is possible for that cation. For all others, only the monoclinic forms for the orthophosphates were observably contaminated by the Pb flux used to dissolve the starting material prior to crystal growth.

In examining the REEPO₄ structures, it is evident that when the REE cation radius contracts beyond a certain point (empirically 1.05 Å), the REE cation becomes too small to maintain the monoclinic structure type, and the structure distorts to a lower density, lower energy, tetragonal structure type. Once this change from monoclinic to tetragonal symmetry has occurred, the divalent lead cation can no longer fit into this confined HREEO₈ polyhedra. The tetragonal orthophosphates are all of the same structure type, with a slight contraction of unit cell volume with increasing atomic number. The same holds true for the monoclinic orthophosphates. There is a dramatic jump in the cell volumes between Gd (276 Å³) and Tb (292 Å³) with the phase change.

The tetravalent lead cation with an ionic radius of 0.94 Å [16], would appear to fit better into the tetragonal xenotime structure orthophosphates with the smaller HREE cations (1.04 Å to 0.87 Å, [16]), but significant Pb was not observed in those samples. Abraham et al. [8], did find some trivalent Pb in their EPR experiments, but other valence states of Pb such as tetravalent lead could have been present since they are not observable by means of EPR spectroscopy [8]. The flux used for crystal growth, Pb₂P₂O₇, derived from the decomposition of PbHPO₄, contains divalent lead thus, it seems more likely that the Pb was in the divalent state under the conditions of synthesis.

Characterizing the exact Pb contamination within a given orthophosphate is problematic because of the degree to which the Pb concentrations vary, not only within a single grain but also from grain to grain. For this reason it is recommended that each laboratory perform systematic x-ray mapping for Pb of their “in house” REE orthophosphates grains to determine the actual extent and variation of Pb contamination in their own mounts. As can be seen in Table 7 (e.g., grain #3), it may be that the Pb contamination is homogeneous enough that some portion or another of the material may be suitable for use as a quantitative standard for major element concentrations of the REE in question. Once the Pb concentration for a homogeneous grain is known and the position noted, the measured Pb can be proportionally subtracted from the ideal REEPO₄ composition and entered into the laboratory’s standard compositional database for general use.

Regarding which REEPO₄ material should be used for P as an EMPA standard, we suggest that one of the tetragonal orthophosphates should be used to minimize any nonstoichiometry introduced by Pb impurities.

4. Conclusions

Due to their qualities of robustness under the electron beam, resistance to oxidation, and REE purity, the REE orthophosphate standards remain a valuable set of standards for EPMA despite significant Pb contamination in at least 7 of the 16 samples examined. Of those with measurable Pb contamination, only the monoclinic CePO₄ and possibly the LaPO₄ and SmPO₄ contain enough Pb to noticeably affect the stoichiometry for use as a primary standard for major element quantitative analysis (approximately 2 % to 4 % relative differences from their theoretical compositions). None of the tetragonal, xenotime structure orthophosphates (Gd-LuPO₄ and ScPO₄ and YPO₄) contain appreciable Pb.

Acknowledgments

Thanks to Tim Teague at the UC Berkeley Petrographic Laboratory for meticulous sample preparation and to all other researchers who pointed out the presence of Pb in these materials.

5. References

- [1] W. O. Milligan, D. F. Mullica, G. W. Beall, and L. A. Boatner, Structural Investigations of YPO_4 , ScPO_4 , and LuPO_4 . *Inorg. Chim. Acta* **60**, 39-43 (1982).
- [2] W. O. Milligan, D. F. Mullica, G. W. Beall, and L. A. Boatner, Structural Investigations of ErPO_4 , TmPO_4 , and YbPO_4 . *Acta Crystallog.* **C39**, 23-24 (1983).
- [3] W. O. Milligan, D. F. Mullica, G. W. Beall, and L. A. Boatner, Structural Investigations of Three Lanthanide Orthophosphates. *Inorg. Chim. Acta* **70**, 133-136 (1983).
- [4] W. O. Milligan, D. F. Mullica, G. W. Beall, and L. A. Boatner, Crystal data for lanthanide orthophosphates with zircon-type structure. *Inorg. Chim. Acta* **77**, L23-25 (1983).
- [5] D. F. Mullica, D. A. Grossie, and L. A. Boatner, Coordination geometry and structural determinations of SmPO_4 , EuPO_4 , and GdPO_4 . *Inorg. Chim. Acta* **109**, 105-110 (1985).
- [6] D. F. Mullica, D. A. Grossie, and L. A. Boatner, Structural refinements of praseodymium and neodymium orthophosphate. *J. Solid State Chem.* **58**, 71-77 (1985).
- [7] L. A. Boatner and B. C. Sales, Monazite in Radioactive Waste Forms for the Future, W. Lutze, R. C. Ewing, eds., Elsevier Science Publishers B.V. (1988) pp. 495-564.
- [8] M. M. Abraham, L. A. Boatner, and M. Rappaz, Novel Measurement of Hyperfine Interactions in Solids: 207Pb^{3+} in YPO_4 and LuPO_4 , *Phys. Rev. Lett.* **45** (10), 839-842 (1980).
- [9] E. Jarosewich and L. A. Boatner, Rare-Earth Element Reference Samples for Electron Microprobe Analysis. *Geostand. Newslett.* Vol XV, 2 (1991).
- [10] M. J. Drake and D. F. Weill, New rare earth element standards for electron microprobe analysis. *Chem. Geol.* **10**, 179-181 (1972).
- [11] P. L. Roeder, Electron-Microprobe Analysis of Minerals for Rare-Earth Elements: Use of Calculated Peak Overlap Corrections. *Can. Mineralog.* **23**, 263-271 (1985).
- [12] P. L. Roeder, D. MacArthur, X. P. Ma, G. R. Palmer, and A. N. Mariano, Cathodoluminescence and microprobe study of rare-earth elements in apatite. *Am. Mineralog.* **72**, 801-811 (1987).
- [13] J. J. Donovan, D. A. Snyder, and M. L. Rivers, An improved interference correction for trace element analysis. *Microbeam Anal.* **2**, 23-28 (1993).
- [14] V. D. Scott and G. Love, Quantitative Electron-Probe Microanalysis, 2nd Ed., Wiley & Sons, New York (1983) p. 105.
- [15] J. I. Goldstein, D. E. Newbury, P. Echlin, D. C. Joy, C. Fiori, and E. Lifshin, Scanning Electron Microscopy and X-Ray Microanalysis, Plenum, New York (1981) p. 436.
- [16] R. D. Shannon, Revised effective ionic radii and systematic studies of interatomic distances in halides and chalcogenides. *Acta Crystallog.* **A32**, 751-767 (1976).

About the authors: John J. Donovan is a research assistant with the University of Oregon, John M. Hancher is a assistant professor of geochemistry at The George Washington University, Phillip M. Picolli is a research scientist at the University of Maryland, Department of Geology, Marc D. Schrier is as staff scientist at Quantum Dot Corporation, Lynn A. Boatner is a corporate fellow in the Solid State Division at Oak Ridge National Laboratory and Eugene Jarosewich is a research chemist (emeritus) at the Department of Mineral Sciences, the Museum of Natural History, Smithsonian Institution.